ELSEVIER

Materials Science and Engineering A212 (1996) 6–13

MATERIALS SCIENCE & ENGINEERING A

Growth mechanism of Cr_2O_3 scales: oxygen and chromium diffusion, oxidation kinetics and effect of yttrium

S.C. Tsai[a], A.M. Huntz[a], C. Dolin[b]

[a]*Laboratoire de Métallurgie Structurale, CNRS URA 1107, Bat 413, Université Paris XI-Orsay, 91405 Orsay, France.*
[b]*Laboratoire de Physique du Solide, Ecole Supérieure de Physique et de Chimie Industrielles de la ville de Paris, 75231 Paris Cedex 05, France.*

Received 31 July 1995; in revised form 28 November 1995

Abstract

The growth mechanism of Cr_2O_3 scales was studied at 900 and 800 °C by determining diffusivities, both in bulk and along the grain boundary, of ^{18}O and ^{54}Cr in Cr_2O_3 scales formed on a $Ni_{70}Cr_{30}$ alloy with and without yttrium implants (10^{16} ions cm^{-2}). The diffusion of ^{18}O and ^{54}Cr was carried out simultaneously which allowed us to obtain a direct comparison of self-diffusion. All the concentration profiles were established by SIMS. Without yttrium in Cr_2O_3 scales, the oxygen bulk diffusion coefficient is close to that of chromium, but the chromium grain boundary diffusion coefficient is greater than that of oxygen. The presence of yttrium in Cr_2O_3 scales slightly decreases the grain boundary diffusivities of ^{18}O and ^{54}Cr, but enhances the oxygen lattice diffusion. The parabolic oxidation constant rates calculated from our diffusion data according to Wagner theory, were close to the experimental ones determined by oxidation kinetic tests. It is concluded that the Cr_2O_3 scale growth is controlled by counter-current diffusion of oxygen and chromium for the unimplanted and implanted alloys, mainly by grain boundary diffusion. Yttrium does not change the growth mechanism.

Keywords: Cr_2O_3 scales; Growth mechanism; Yttrium; ^{18}O and ^{54}Cr diffusion; Oxidation kinetics

1. Introduction

Cr_2O_3 scales are frequently formed on the surface of the chromium-bearing alloys at high temperatures to protect the alloys. As a consequence, it is very interesting to study the growth mechanism of Cr_2O_3 scales. Moreover, the addition of active elements such as yttrium to the alloys is well known to increase the adherence of protective Cr_2O_3 scales and improve the oxidation resistance of the alloys. Many attempts have been made in order to understand the growth mechanism of Cr_2O_3 scales and the effect of yttrium. One of these fundamental studies consists of determining diffusion coefficients of oxygen and chromium in Cr_2O_3.

From first studies, it was shown that oxygen diffusion was slower than chromium diffusion by about 3 orders of magnitude [1]. Later, from oxidation studies, it was concluded that the Cr_2O_3 scales on the chromium metal grow by counter-current diffusion of chromium and oxygen, mainly via the grain boundary [2,3]. It was then suggested that outward cationic diffusion is more important for the growth of undoped Cr_2O_3 scales [4,5]. On the contrary, Sabioni et al. [6–8] determined recently the bulk and grain boundary self-diffusion coefficients of oxygen and chromium in single crystals and in massive polycrystals of Cr_2O_3 in a temperature range of 1100–1450 °C and showed that the oxygen diffusion coefficients are greater than those of chromium. This agrees with the results obtained by King et al. [9]. However, the oxygen and chromium diffusion coefficients of Sabioni are too small to account for the growth rate of Cr_2O_3 scales using Wagner's theory.

In the literature, it appears that the values of oxygen and chromium diffusion coefficients determined in single crystals are some orders of magnitude smaller than the data obtained on polycrystalline materials or on scales. In order to clarify this discrepancy, a new analysis of the diffusion profiles in the case of polycrystalline Cr_2O_3 was used in an earlier work [10,11]: the first part of the penetration profiles corresponds to an apparent diffusion, and the second part is related to grain boundary diffusion. Moreover, considering the surface

PII S0921-5093(96)10173-8

roughness of Cr_2O_3 scales, a ridge model was proposed to modify the f value, the fraction of sites associated with grain boundary. The modified f value becomes smaller than that generally calculated with the classical formula $f = 3\delta/\Phi$ (δ:grain boundary width and Φ: grain size) which is applied for smooth surface samples, for instance massive polycrystals of Cr_2O_3. With these two modifications for analyzing the diffusion profiles, oxygen bulk diffusion coefficients of single crystals and polycrystalline materials are similar. Moreover oxygen bulk diffusion coefficients in Cr_2O_3 scales are close to those determined in massive Cr_2O_3 (single crystals and massive polycrystals).However, oxygen grain boundary diffusion coefficients in scales are slightly greater than those in massive polycrystals, probably on account of the differences in the chemistry or/and structure of the grain boundaries [11].

It is often suggested that the presence of yttrium in chromia former alloys allows a change in the growth mechanism of Cr_2O_3 scales from one involving predominant cation diffusion to one involving predominant anion diffusion due to the segregation of yttrium to the grain boundaries [12–16]. It is also suggested that the presence of yttrium can form Cr_2O_3 scales which act as a better diffusion barrier [17]. Until now, there has not been a lot of diffusion data to confirm the effect of yttrium on the atomic transport in Cr_2O_3 scales.

In our present work, two approaches are used to study the growth mechanism of Cr_2O_3 sacles and the effect of yttrium: Firstly, at 900, 800 °C and p_{O_2} = 0.1atm, following the same analysis of diffusion profiles as mentioned previously [10, 11], the diffusion experiments are destined to determine the diffusion coefficients, in bulk (D_B) and along grain boundary (D_{gb}), of oxygen and chromium in Cr_2O_3 scales formed on a $Ni_{70}Cr_{30}$ alloy unimplanted and implanted with yttrium. Secondly, by oxidation kinetic tests, the parabolic oxidation constant rate (k_c) is determined on the unimplanted and implanted alloys in a thermobalance. This experimental k_c value is then compared with the calculated one from the diffusion data in order to understand the growth mechanism of Cr_2O_3 scales. All the diffusion profiles are established by secondary ion mass spectrometry (SIMS) which is the most accurate modern technique for measuring diffusion profiles on a small depth.

2. Experimental method

Materials: The Cr_2O_3 scales were formed by oxidation of a $Ni_{70}Cr_{30}$ alloy elaborated by CECM, CNRS (Vitry, France): 68.4 wt% Ni, 31.6 wt% Cr (analysis by EDAX). The impurities in the alloy are 0.2wt% Si, 500ppm Fe, 500ppm Ca and 150ppm Al (analysed in CECM Vitry, France). Before oxidation, all samples were cold rolled (40%), preannealed for 15h at 900 °C in argon, and then polished to 1200 mesh grit SiC. The implantation of yttrium (10^{16} ions cm^{-2} with the energy equal to 150keV) is carried out in CSNSM (Orsay, France). By SIMS analysis, the maximum concentration of yttrium is located about 7nm beneath the surface of the alloy and the presence of yttrium is found in scales formed on the implanted alloy. High purity $^{18}O_2$ gas and ^{54}Cr (purity higher than 96%) used as stable tracers were obtained from the Commissariat à l'Energie Atomique (France). As shown in Fig. 1, the scales with and without yttrium are compact, made of Cr_2O_3 with very small amounts of Ni, Si, Al and Ca; the average grain size of the oxide scales are shown in Tables 1 and 2.

Oxidation kinetic tests: These tests for the unimplanted and implanted $Ni_{70}Cr_{30}$ alloys were carried out in a SETARAM thermobalance at 900 and 800 °C in

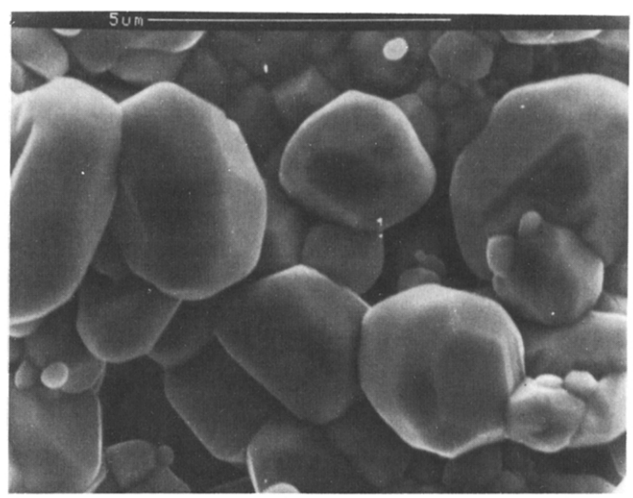

(a)

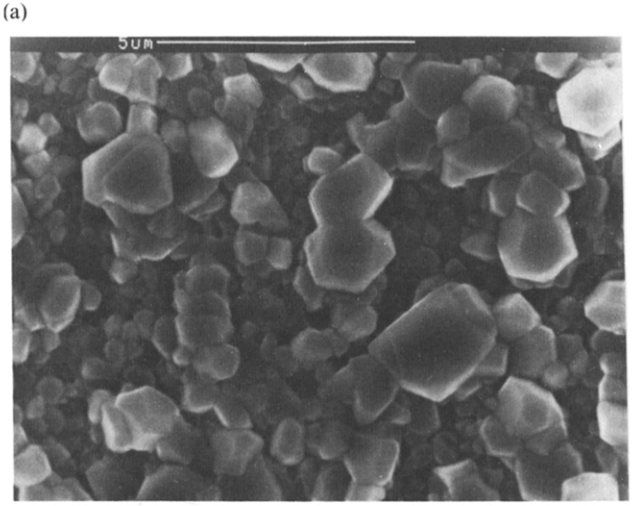

(b)

Fig. 1.(a) SEM micrograph of the scale surface formed on the unimplanted alloy at 900 °C, 165 h and p_{O_2} = 1 atm. (b) SEM micrograph of the scale surface formed on the implanted alloy at 900 °C, 100 h and p_{O_2} = 1 atm.

Table 1
Experimental conditions of ^{18}O and ^{54}Cr diffusion in Cr_2O_3 scales formed on the unimplanted alloy

Sample	Experimental conditions	Φ (μm)
Cr900	^{16}O, 1 atm, 900 °C, 165 h + cooling (80 °C h^{-1}) +	2
O900	^{54}Cr layer + ^{18}O, 0.1 atm, 900 °C, 2 h	
Cr800	^{16}O, 1 atm, 900 °C, 165 h + cooling (80 °C h^{-1}) +	2
O800	^{54}Cr layer + ^{18}O, 0.1 atm, 800 °C, 2.5 h	

different atmospheres of oxygen: 0.25, 1atm, 2atm. Before each test, the samples were finally polished with 1200 mesh grit SiC, and were ultrasonically cleaned in aceton, then washed with ethanol.

Experimental diffusion conditions: The oxygen and chromium diffusion was studied by means of ^{18}O–^{16}O and ^{54}Cr–^{52}Cr isotopic exchange respectively. For simultaneous oxygen and chromium diffusion, the samples were first oxidized in $^{16}O_2$ and cooled to room temperature. Then, a ^{54}Cr layer was deposited on the sample surface by evaporation at a total pressure equal to 10^{-4} Pa. The samples were then heat-treated in $^{18}O_2$. The average thickness of ^{54}Cr tracer deposited was about 15nm analysed by SIMS. It was verified that the cooling rate at 240 °C h^{-1} or 80 °C h^{-1} does not induce any modification of the diffusion [11]. All diffusion experimental conditions of the samples are given in Tables 1 and 2. It is suggested that equilibrium with the gas and temperature in the low depth concerning the diffusion zone can be obtained as soon as the diffusion starts [11]. So, all comparisons between samples are allowed.

Analysis of the diffusion profiles of ^{18}O and ^{54}Cr: For all experiments, the concentration profiles were established by SIMS (CAMECA/IMS 4F), using a 10keV Cs^+ ion source for oxygen and a 10keV O^+ ion source for chromium. The scanned area was 250 × 250 μm and the analyzed zone was 62 μm in diameter. The sputtering rate was determined by measuring the crater depth with a profilometer.

Determination of the diffusion coefficients: To determine oxygen diffusion coefficient, the Fick solution given for constant surface concentration was used:

$$\frac{C(x)-C_s}{C_0-C_s}=\mathrm{erf}\left(\frac{x}{\sqrt{Dt}}\right) \quad (1)$$

with C_0, the tracer natural concentration in the sample, equal to 0.2%, C_s, the tracer constant surface concentration and t, diffusion time.

A thin film method solution was used to determine chromium diffusion coefficients:

$$C(x)=C_0\exp\left(-\frac{x^2}{4Dt}\right) \quad (2)$$

As it was considered that diffusion of oxygen and chromium occurs in a B regime: $\delta \ll \sqrt{D_B t} \ll \Phi$[10], the first part of the oxygen and chromium penetration profiles can determine the apparent diffusion coefficient (D_{app}); it means that D in Eqs. (1) and (2) is considered as D_{app}whose definition is given by Hart [18]:

$$D_{app}=(1-f)D_B+D_{gb} \quad (3)$$

where D_B is the bulk diffusion coefficient, and D_{gb} is the grain boundary diffusion coefficieny.

In the second part of the profiles corresponding to grain boundary diffusion, as the values of β ($\simeq D_{gb}\cdot\delta / D_B\cdot 2(D_B t)^{1/2}$)are greater than 10. D_{gb} can be determined by the following equation proposed by Wipple-Le Claire [19]:

$$D_{gb}\cdot\delta=0.661\cdot(-P_{gb})^{-5/3}\cdot(4D_B/t)^{1/2} \quad (4)$$

where P_{gb} is the slope of the curve $\ln C=f(x^{6/5})$ plotted in the second part of the experimental profiles. Taking $\delta=10^{-7}$cm and combining Eqs. (3) and (4), a second order equation with an unknown D_B is obtained:

$$(1-f)D_B+1.332\cdot10^7\cdot f\cdot(-P_{gb})^{-5/3}\cdot(t)^{-1/2}\cdot(D_B)^{1/2}-D_{app}=0 \quad (5)$$

Using Eq. (5), D_B can be calculated, then D_{gb} can be determined using Eq. (4).

Here, f has been modified by the ridge model and can be expressed for a rough surface by [11]:

$$f=\frac{\frac{\Phi}{2}}{\frac{\Phi}{2}+2R_a}\cdot\frac{3\delta}{\Phi}$$

R_a: roughness of the scale surface (about 1 μm in this case).

3. Results

3.1. Diffusion experiments

Some oxygen and chromium penetration profiles are shown in Figs. 2–4. As the diffusion experiments of oxygen and chromium are carried out simultaneously, it is possible to make a direct comparison with both diffusions. The results of the oxygen and chromium diffusion coefficients determined in Cr_2O_3 scales formed on the unimplanted and implanted alloys are presented in Table 3.

Table 2
Experimental conditions of ^{18}O and ^{54}Cr diffusion in Cr_2O_3 scales formed on the implanted alloy

Sample	Experimental conditions	Φ (μm)
Cr900Y	Y implantation + ^{16}O, 1 atm, 900 °C, 100 h + cooling (240 °C h^{-1}) +	1
O900Y	^{54}Cr layer + ^{18}O, 0.1 atm, 900 °C, 4 h	
Cr800Y	Y implantation + ^{16}O, 1 atm, 800 °C, 100 h + cooling (240 °C h^{-1}) +	0.5
O800Y	^{54}Cr layer + ^{18}O, 0.1 atm, 800 °C, 7 h	

3.1.1. Oxygen and chromium diffusion coefficient in Cr_2O_3 scales without yttrium (Table 3)

The oxygen D_B values at 900 and 800 °C are equal to 4.4×10^{-17} and $2.6 \times 10^{-18} cm^2 s^{-1}$. The oxygen D_{gb} values at 900 and 800 °C are 1.6×10^{-12} and 5.9×10^{-13} $cm^2 s^{-1}$ in Cr_2O_3 scales. The chromium D_B values are equal to 2.0×10^{-17} and 5.9×10^{-18} $cm^2 s^{-1}$ at 900 and 800 °C, not far from the oxygen D_B values. But the chromium D_{gb} values at these two temperatures are equal to 9.3×10^{-12} and $1.1 \times 10^{-12} cm^2 s^{-1}$ respectively, greater than our oxygen D_{gb} values. All D_{app}, D_B and D_{gb} values of oxygen and chromium are presented in Fig. 5. According to our results, without the presence of yttrium in scales, chromium bulk diffusion is close to that of oxygen, and chromium grain boundary diffusion is faster than that of oxygen, especially at 900 °C.

3.1.2. Oxygen and chromium diffusion coefficient in Cr_2O_3 scales with yttrium

With the presence of yttrium in scales, except oxygen D_B values, most of oxygen and chromium diffusivities become smaller than those determined in scales without yttrium. As shown in Fig. 6 and Table 3, oxygen D_B values are greater than chromium D_B values, but chromium D_{gb} values are still greater than those of oxygen at 900 °C, as in the former case without the presence of yttrium.

Our diffusion results show that, though chromium diffusion is decreased due to the presence of yttrium, chromium grain boundary diffusion is still greater than that of oxygen. As the grain boundary diffusion is very important for scale growth, chromium diffusion must be considered as well as oxygen diffusion in studying the effect of yttrium on the mechanism of Cr_2O_3 scale growth.

3.2. Oxidation kinetic tests

Representative kinetic curves for the oxidation of the $Ni_{70}Cr_{30}$ alloy in various oxygen pressures at 900 and 800 °C are shown in Fig. 7. The curves generally obey a parabolic rate law: $(\Delta m s^{-1})^2 = k_p t$. The k_c values ($cm^2 s^{-1}$) defined as $x^2 = k_c t$ (x: oxide thickness) are obtained by:

$$k_c = \left(\frac{M_{Cr_2O_3}}{3 M_O \rho_{Cr_2O_3}} \right)^2 k_p$$

All the k_c values are given in Table 4. A p-type conductivity behavior is observed in our Cr_2O_3 scales because k_c becomes greater when the oxygen pressure is higher. As a consequence, it can be suggested that the main point defect is either oxygen interstitial (O_i'') or chromium vacancy (V_{Cr}'''), or both. The implantation of yttrium in the alloy decreases the oxidation rate of the alloy: the k_c value determined on the implanted alloy becomes smaller than that determined on the unimplanted alloy (Fig. 7 and Table 4). The k_c values for $p_{O_2} = 0.1$atm were estimated from the experimental values of Table 4 and are given in Table 5. It indicates that the k_c values at 900, 800 °C and $p_{O_2} = 0.1$atm are

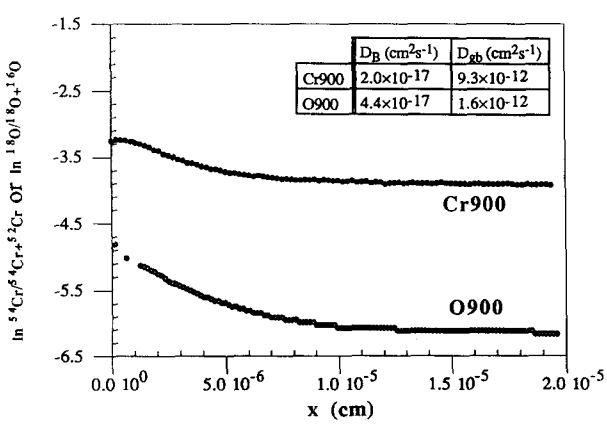

Fig. 2. Oxygen and chromium diffusion profiles in scales formed on the unimplanted alloy at 900 °C, $p_{O_2} = 0.1$ atm and $t_{diff} = 2$ h.

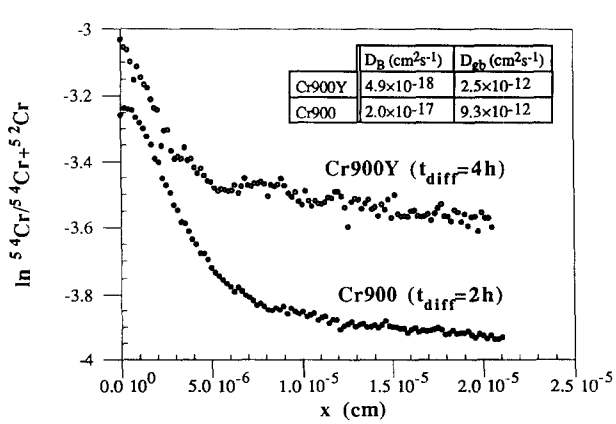

Fig. 3. Chromium diffusion profiles in scales formed on the unimplanted and implanted alloy.

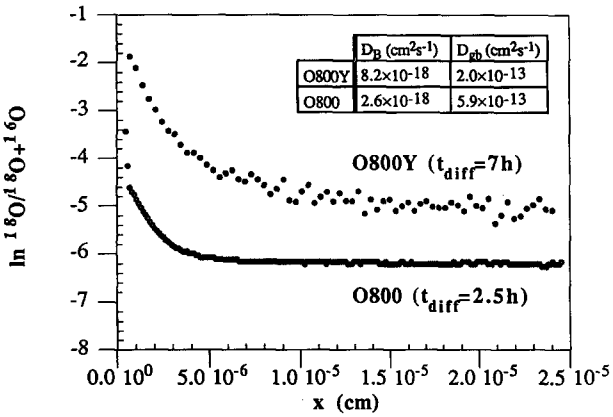

Fig. 4. Oxygen diffusion profiles in scales formed on the unimplanted and implanted alloy.

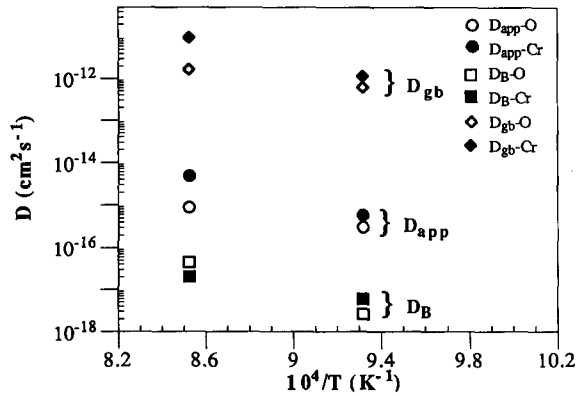

Fig. 5. D_{app}, D_B and D_{gb} values of oxygen (white symbols) and chromium (dark symbols) determined in Cr_2O_3 scales formed on the unimplanted alloy.

equal to 4.4×10^{-14} and 2.0×10^{-14} cm^2s^{-1} for the unimplanted alloy, and 3.0×10^{-14} and 4.6×10^{-15} cm^2s^{-1} for the implanted alloy respectively.

4. Discussion

4.1. Diffusion

Concerning the analysis of the diffusion data, it must be remarked that the isotope diffusion occurs in a scale whose composition is not homogeneous. Indeed, the scale is subjected to a chemical potential gradient which may correspond to a variation in the defect concentrations. Nevertheless diffusion experiments were made with various diffusion times, i.e. various penetration depths and the deduced diffusion coefficients are of the same order of magnitude. Another important point concerns the fact that the diffusion coefficients do not depend on the previous oxidation time, i.e. on the initial oxide thickness and/or the initial shape of the chemical potential gradient [11]. These results indicate that, in the present case, it is permissible to use a model that implies that the scale has a homogeneous composition for analysing the penetration profiles.

Table 3
D_{app}, D_B and D_{gb} (cm^2 s^{-1}) of ^{18}O and ^{54}Cr determined in scales at $p_{O_2} = 0.1$ atm

Sample	f	D_{app}	D_B	D_{gb}
O900	0.0005	8.6×10^{-16}	4.4×10^{-17}	1.6×10^{-12}
Cr900		4.7×10^{-15}	2.0×10^{-17}	9.3×10^{-12}
O900Y	0.0006	6.6×10^{-16}	1.6×10^{-16}	8.3×10^{-13}
Cr900Y		1.5×10^{-15}	4.9×10^{-18}	2.5×10^{-12}
O800	0.0005	3.0×10^{-16}	2.6×10^{-18}	5.9×10^{-13}
Cr800		5.8×10^{-16}	5.9×10^{-18}	1.1×10^{-12}
O800Y	0.00065	1.4×10^{-16}	8.2×10^{-18}	2.0×10^{-13}
Cr800Y		1.7×10^{-16}	2.4×10^{-18}	2.5×10^{-13}

4.1.1. Scales without presence of yttrium

In our earlier work [11], only oxygen diffusion coefficient was determined because, at that time, there was no ^{54}Cr layer on the surface of Cr_2O_3 scales. Results show that the oxygen D_B value determined in single crystals, massive polycrystals and scales at 900 °C is about 10^{-17} cm^2s^{-1}, close to our oxygen D_B value in this work. It means that oxygen diffusion is not perturbed by the chromium layer. The Figs. 8 and 9 respectively show our oxygen and chromium diffusion coefficients in this work and those determined by other workers.

Considering Fig. 8 relative to oxygen diffusion, it appears that D_B values determined in massive polycrystals by Sockel et al. [20] and D_B values extrapolated from Sabioni et al. [7] are close to our D_B values. The isotropic diffusion coefficient determined in scales by Graham et al. [21] is in fact an apparent one. For oxygen grain boundary diffusion coefficient, our D_{gb} values are in good agreement with those of Graham in scales [21], but greater than those determined in massive polycrystals by Sockel [20]. It appears that oxygen D_{gb} values determined in Cr_2O_3 scales are greater than those

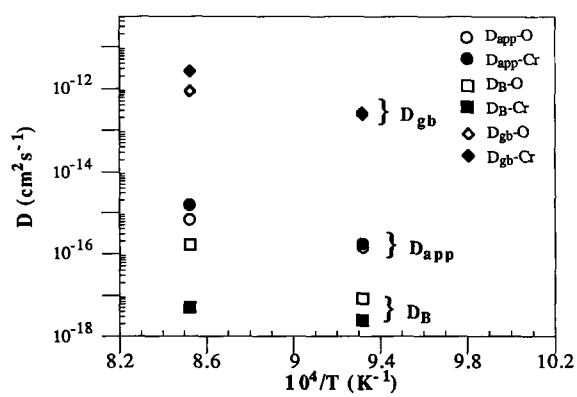

Fig. 6. D_{app}, D_B and D_{gb} values of oxygen (white symbols) and chromium (dark symbols) determined in Cr_2O_3 scales formed on the implanted alloy.

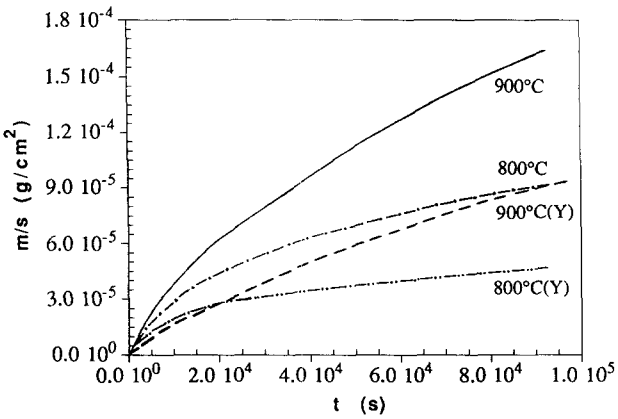

Fig. 7. Oxidation kinetic curves of the unimplanted and implanted alloys at 900 °C, 800 °C and $p_{O_2} = 1$ atm.

determined in massive polycrystals, probably due to the more easy diffusion paths in scales on account of differences in the grain boundary microchemistry and microstructure.

For chromium diffusion coefficient, as shown in Fig. 9, it appears that the data are very scattered when considering our values and those of Sabioni [6], Hagel [22], Lobnig [23] and Atkinson [24]. From Sabioni's work, the chromium extrapolated D_{gb} value at 900 °C is very close to his extrapolated chromium D_B value [8]. This was rather surprising and is related to the fact that Sabioni found an activation energy for grain boundary diffusion that is greater than the bulk diffusion activation energy. Lobnig et al.[23] determined chromium bulk diffusion coefficients in Cr_2O_3 scales whose order of magnitude is about $10^{-15}cm^2s^{-1}$ at 900 °C. This is close to our D_{app} values (Table 3), thus bigger than our D_B values, possibly because they did not consider the effect of apparent diffusion in the first part of their oxygen concentration profiles.

It appears that there is a great difference between our chromium D_B and D_{gb} values and some extrapolated values determined by other workers. This is firstly due to the different analysis for the first part of the diffusion profiles: while apparent diffusion is considered in our case, bulk diffusion was only taken into account by other authors. Secondly, the extrapolated values were obtained on the basis of few points, which may lead to a great uncertainty. Finally, the microchemistry of the grain boundaries can vary with the temperature and the material purity.

Table 4
k_c ($cm^2\ s^{-1}$) determined on the alloy $Ni_{70}Cr_{30}$ implanted and unimplanted in different oxygen pressure at 900 and 800 °C

p_{O_2} (atm)	0.25 atm	1 atm	2 atm
k_c (900)	5.2×10^{-14}	8.9×10^{-14}	2.4×10^{-13}
k_c (900-Y)	3.3×10^{-14}	4.0×10^{-14}	5.2×10^{-14}
k_c (800)	2.7×10^{-14}	3.3×10^{-14}	1.1×10^{-13}
k_c (800-Y)	5.0×10^{-15}	6.3×10^{-15}	7.2×10^{-15}

In the case of chromium scales undoped by yttrium, it will be retained that the growth is controlled by preferential grain boundary diffusion of chromium, but oxygen grain boundary diffusion is not negligible. Nevertheless, formation of new oxide within the scale can be excluded [25] taking into account the nature of the point defects probably responsible for the scale growth. Indeed, the scale growth depends on the oxygen pressure [11]: the growth rate increases with the oxygen pressure and this means that the main defects responsible for diffusion of the anion and cation must be O_i'' and V_{Cr}''' respectively. If a new oxide was formed within the scale, then according to Basu et al. [26], the ^{18}O profiles would show a peak inside the scale. It is not the case in our experiments. So, our feeling is that oxide growth occurs only at the inner and outer interface. This is also supported by the fact that the scales are flat, they do not show any convolutions and ridges as frequently observed on alumina scales. This is in agreement with the fact that growth stresses determined in such scales are of minor importance [27].

4.1.2. Scales with presence of yttrium

It is often suggested that oxygen diffusion becomes predominant during Cr_2O_3 scales growth with the presence of yttrium to grain boundary which is expected to reduce chromium grain boundary diffusion. This leads to a change in the growth mechanism of Cr_2O_3 scales. But, as mentioned in Przybylski's work [12], it seems unlikely that the segregation of yttrium to chromia grain boundaries would decrease cation flux and at the same time increase anion flux. In agreement with this idea, our results show that the chromium D_{gb} value is decreased, but the oxygen D_{gb} value is also decreased

In sintered polycrystals of Cr_2O_3 and Cr_2O_3 – 0.09%Y_2O_3, W.E. King et al. [28,29] determined chromium and oxygen diffusion coefficient at 1100 °C and at the oxygen partial pressure corresponding to that of the Cr/Cr_2O_3 equilibrium at that temperature. Their results indicate that, in these undoped and doped materials, oxygen diffusion in the bulk, as well as in grain boundaries, is significantly faster than chromium diffusion. It also appears that the effect of yttrium increases oxygen bulk diffusion by a factor of 20 and decreases oxygen grain boundary diffusion by a factor of 20. Our results concerning oxygen diffusion do not agree with those of King et al. They are also in agreement with results concerning diffusion in Al_2O_3 by Le Gall et al. [30]. Those authors found that yttrium increases oxygen bulk diffusion and decreases oxygen grain boundary diffusion. There are no data concerning cation diffusion in doped Al_2O_3.

Thus it can be concluded that a yttrium presence in Cr_2O_3 scales decreases the diffusivity of both anions

Table 5
k_c ($cm^2\ s^{-1}$) calculated from diffusion data for $Ni_{70}Cr_{30}$ unimplanted and implanted with yttrium, compared to the k_c value estimated by oxidation kinetic tests

Diffusion mechanism		Bulk diffusion	Grain boundary diffusion	Apparent diffusion	Estimated k_c value
k_c (900)	unimplanted	4.2×10^{-16}	8.4×10^{-11}	4.3×10^{-14}	4.4×10^{-14}
	implanted	9.9×10^{-16}	2.5×10^{-11}	1.6×10^{-14}	3.0×10^{-14}
k_c (800)	unimplanted	6.3×10^{-17}	1.2×10^{-11}	6.4×10^{-15}	2.0×10^{-14}
	implanted	6.8×10^{-17}	3.2×10^{-12}	2.2×10^{-15}	4.6×10^{-15}

and cations and does not change the growth mechanism. The decrease of the grain boundary diffusion must be due to yttrium segregation or precipitation in grain boundaries as the solubility of this active element in chromia must be very low (for instance 10 mol ppm in Al_2O_3 at 1550 °C [31]). The increase of oxygen D_B by yttrium can be due to the donor effect of this element. Indeed, by EXAFS, Loudjani et al. [31] showed that yttrium in alumina gives defect complexes $[Y_{Al}^{x} + mV_O^{\cdot} + nO_i'']^{2(m-n)}$ with $m > n$. The question then being why is chromium D_B not increased if the defects responsible for chromium diffusion are chromium vacancies. But, the doping of the scale by yttrium can induce a modification of the nature or amount of other impurities which can be incorporated in the scale. In order to detect the distribution of both yttrium and other impurities within the Cr_2O_3 scales, STEM analyses are in progress.

4.2. Oxidation kinetics

It was found that the k_c values determined on the implanted alloy is smaller than those determined on the unimplanted alloy. At present, this difference is attributed to the segregation and precipitation of yttrium in grain boundaries of Cr_2O_3 scales [12,13] which decreases oxygen and chromium grain boundary diffusion.

From the classical equation given by Wagner which relates the parabolic oxidation constant k_c to the diffusion coefficients for an oxide M_aO_b, k_c can be expressed:

$$k_c(\text{calc.}) = \int_{p_{O_2}^{int}}^{p_{O_2}^{ext}} \left[D_{anion} + \frac{b}{a} D_{cation} \right] d\ln(p_{O_2})$$

$p_{O_2}^{ext}$: oxygen pressure at the gas/scale interface; $p_{O_2}^{int}$: oxygen pressure at the alloy/scale interface and D_{anion} and D_{cation}: anion and cation diffusion coefficients.

This equation only applies to oxidation governed by a flux of species perpendicular to the surface and can be used provided that lateral growth does not occur. In our case, as said previously, lateral growth and growth within the scale were excluded. In this equation, the diffusion coefficients that must be taken into account are the apparent diffusion coefficients D_{app} (Eq. (3)), since all diffusion paths contribute to the scale growth.

Writing $D = D^{\circ}(p_{O_2})^n$ for each species (D° being the diffusion coefficient at $p_{O_2} = 1$atm) and considering that self-diffusion occurs by O_i'' and V_{Cr}''':

$$\begin{aligned} k_c &= \int D_O^{\circ}(p_{O_2})^{1/6} d\ln(p_{O_2}) + \frac{3}{2}\int D_{Cr}^{\circ}(P_{O2})^{3/16} d\ln(p_{O_2}) \\ &= 6D_O^{\circ}(p_{O_2}^{ext})^{1/6} + 8D_{Cr}^{\circ}(p_{O_2}^{ext})^{3/16} \\ &= 6D_O^{\circ}(0.1\text{atm}) + 8D_{Cr}^{\circ}(0.1\text{atm}) \end{aligned} \quad (6)$$

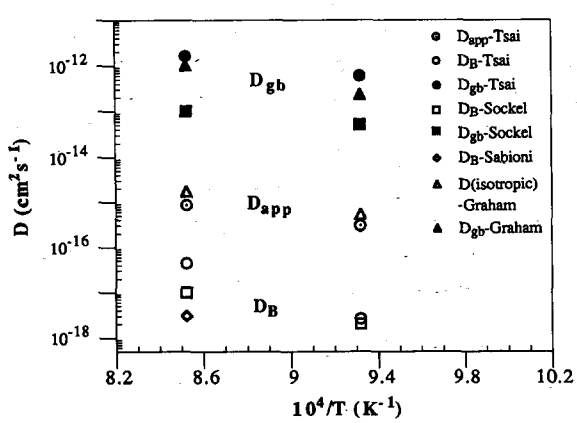

Fig. 8. Oxygen D_{app}, D_B and D_{gb} values determined in this work and those found in the literature for "undoped" Cr_2O_3.

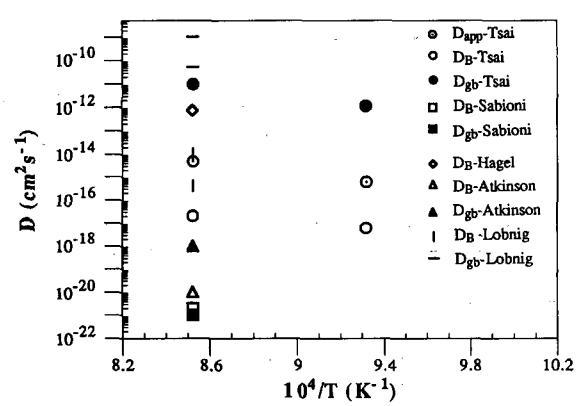

Fig. 9. Chromium D_{app}, D_B and D_{gb} values determined in this work and those found in the literature for "undoped" Cr_2O_3.

Table 6
The values of the terms 6 D_{app}^{O} and 8 D_{app}^{Cr} compared with the estimated k_c values ($cm^2\ s^{-1}$)

		6 D_{app}^{O}	8 D_{app}^{Cr}	Estimated
900 °C	unimplanted	5.2×10^{-15}	3.8×10^{-14}	4.4×10^{-14}
	implanted	4.0×10^{-15}	1.2×10^{-14}	3.0×10^{-14}
800 °C	unimplanted	1.8×10^{-15}	4.6×10^{-15}	2.0×10^{-14}
	unimplanted	8.4×10^{-16}	1.4×10^{-15}	4.6×10^{-15}

Taking the D_{app} values of oxygen and chromium, the parabolic oxidation constants were calculated and reported in Table 5. These values agree with the k_c values estimated from experimental tests. It clearly appears, by comparison of the order of magnitude of the estimated k_c values with the calculated k_c values on the basis of bulk or grain boundary diffusion, that *the scale growth is dominated by counter-current diffusion of oxygen and chromium by both the bulk and the grain boundary, the main phenomenon being grain boundary diffusion.* Indeed, if the k_c value is calculated by considering only the D_B values, then the calculated k_c values are much smaller than the experimental ones. Moreover, since the chromium D_{app} value is always greater than that of oxygen, the term 8 D_{app}^{Cr} in Eq. (6) is greater than the term 6 D_{app}^{O}, as shown in Table 6. So, the chromium diffusion is more important than that of oxygen for the Cr_2O_3 growth for both undoped and yttrium doped scales.

5. Conclusion

The growth mechanism of Cr_2O_3 scales at 900 and 800 °C is studied by determining oxygen and chromium diffusivities and oxidation kinetics; the effect of yttrium is also studied. From our results, it can be concluded that:

1. Without presence of yttrium in Cr_2O_3 scales, chromium diffusion is faster than oxygen diffusion, except for bulk diffusion at 900 °C.
2. The presence of yttrium in scales enhances oxygen bulk diffusion but decreases oxygen grain boundary diffusion. It also reduces the bulk and grain boundary diffusion of chromium.
3. With yttrium in scales, chromium grain boundary diffusion is still faster than that of oxygen.
4. Yttrium does not induce a change in the growth mechanism.
5. The implantation of yttrium to the $Ni_{70}Cr_{30}$ alloy decreases the oxidation rate of the alloy.
6. By comparing the experimental k_c values with those calculated from diffusion data, it appears that the Cr_2O_3 scale growth must be controlled by counter-current diffusion of chromium and oxygen for the unimplanted and implanted alloy, mainly by grain boundary diffusion.

References

[1] P. Kofstad, *Non-Stoichiometry, Diffusion and Electrical Conductivity in Binary Metal Oxide*, Wiley, New York (1972).
[2] P. Kofstad and K.P. Lillerud, *J. Electrochem. Soc., 127* (1980) 2410.
[3] K.P. Lillerud and P. Kofstad, *J. Electrochem. Soc., 127* (1980) 2397.
[4] P. Kofstad, *High Temperature Corrosion*, Elsevier, Barking, (1988).
[5] A. Atkinson, *Rev. Mod. Phys., 57* (1985) 437.
[6] A.C.S. Sabioni, B. Lesage, A.M. Huntz, J.C. Pivin and C. Monty, *Philos. Mag. A, 66* (1992) 333.
[7] A.C.S. Sabioni, A.M. Huntz, F. Millot and C. Monty, *Philos. Mag. A, 66* (1992) 351.
[8] A.C.S. Sabioni, A.M. Huntz, F. Millot and C. Monty, *Philos. Mag. A, 66* (1992) 361.
[9] W.E. King and J.H. Park, *Proceedings of the Materials Research Society Spring Meeting* (1988).
[10] A.M. Huntz and S.C. Tsai, *Mater. Sci. Letter, 13* (1994) 821.
[11] S.C. Tsai, A.M. Huntz and C. Dolin, *Oxid. Met., 43* (1995) 581.
[12] K. Przybylski, A.J. Garratt-Reed and G.J. Yurek, *J. Electrochem. Soc., 135* (1988) 509.
[13] K. Przybylski and G.J. Yurek, *J. Electrochem. Soc., 135* (1988) 517.
[14] C.M. Cotell, G.J. Yurek, R.J. Hussey, D.F. Mitchell and M.J. Graham, *Oxid. Met., 34* (1990) 173.
[15] C.M. Cotell, G.J. Yurek, R.J. Hussey, D.F. Mitchell and M.J. Graham, *Oxid. Met., 34* (1990) 201.
[16] M.J. Bennett, H.E. Bishop, P.R. Chalker and A.T. Tuson, *Mater. Sci. Eng., 90* (1987) 177.
[17] D.N. Braski, P.D. Goodell, J.V. Cathcart and R.H. Kane, *Oxid. Met., 25* (1986) 29.
[18] E.W. Hart, *Acta Metall., 5* (1957) 597.
[19] A.D. Le Claire, *J. Appl. Phys., 14* (1963) 351.
[20] H.G. Sockel, B. Saal and M. Heilmaier, *Surface and Interface Analysis, 12* (1988) 531.
[21] M.J. Graham, J.I. Elridge, D.F. Mitchell and R.J. Hussey, *Material Science Forum, 43* (1989) 207, Trans Tech, Switzerland.
[22] W.C. Hagel and A.U. Seybolt, *J. Electrochem. Soc., 108* (1961) 1146.
[23] R.E. Lobnig, H.P. Schmidt, K. Henneses and H.J. Grabke, *Oxid. Met., 37* (1992) 81.
[24] A. Atkinson and R.I. Taylor, NATO *Adv. Study Inst. Ser. B, 129* (1984) 285.
[25] A. Atkinson, *Corr. Sci., 22* (1982) 347.
[26] S.N. Basu and J.W. Halloran, *Oxid. Met., 27* (1987) 143.
[27] S. Daghigh, J.L. Lebrun and A.M. Huntz, *Journée d'automne de la SF2M* , Paris, 1995.
[28] W.E. King and J.H. Park, *Colloq. Phys., 51* (1991) c1551.
[29] J.H. Park, W.E. King and S.J. Rothman, *J. Electrochem. Soc., 70* (1987) 880.
[30] M. Le Gall, A.M. Huntz, B. Lesage, C. Monty and J. Bernardini, *J. Mater. Sci., 30* (1995) 201.
[31] M.K. Loudjani, A.M. Huntz and R. Cortès, *J. Mater. Sci., 28* (1993) 6466.